Astron. Astrophys. 362, 245–254 (2000)

ASTRONOMY AND ASTROPHYSICS

The δ Scuti star θ Tucanae

III. Observational guidelines for mode identification⋆

M. Paparó[1] **and C. Sterken**[2,⋆⋆]

[1] Konkoly Observatory, P.O. Box 67, 1525 Budapest XII, Hungary
[2] University of Brussels (VUB), Pleinlaan 2, 1050 Brussels, Belgium

Received 29 March 2000 / Accepted 11 August 2000

Abstract. On the basis of almost 2000 *b*, *y* photoelectric observations of θ Tucanae collected in an international campaign at two sites and of almost 1500 *v*, *u* observations collected at one site, observational guidelines for mode identification have been searched. Not only the generally used plane (A_{b-y}/A_y versus ϕ_{b-y} - ϕ_y) but each combination of the nonadiabatic observables including amplitude ratio vs. amplitude ratio and phase difference vs. phase difference planes were checked for guidelines. Especially A_b/A_y amplitude ratio and ϕ_{b-y} - ϕ_b phase difference proved to be useful criteria for mode separation in the case of θ Tucanae. The 10 pulsational frequency values published previously by Paparó et al. (1996) are distributed in three groups according to A_b/A_y and in two distinct levels according to ϕ_{b-y} - ϕ_b. The groups consist of closely spaced frequencies. Group III (15.86, 15.94 and 17.06 cycles/day) displays a higher, distinct level than the others according to the A_{b-y}/A_y amplitude ratio and unusual behaviour in *u* colour. Although the discriminative plane does not give the exact value of quantum numbers but predicts which theoretical modes must share the same behaviour. Calibration of the pure observational guidelines by new, delicate theoretical calculation for planes of nonadiabatic observables concerning the location of theoretical modes is urged.

Key words: stars: individual: θ Tuc = HR 139 – stars: oscillations – stars: variables: δ Sct – stars: variables: general – stars: binaries: spectroscopic

1. Introduction

A successful identification of modes excited in δ Scuti stars could make them suitable for asteroseismological investigations since both radial and nonradial modes are excited. The problem of mode identification in δ Scuti stars is definitely situated on the meeting point of observational and theoretical investigation. From theoretical point of view the problem is not so simple as in the case of the Sun and white dwarfs where the high-order modes obey the asymptotic theory which predicts the systematic arrangement of excited modes. The excited modes in δ Scuti stars are of low-order and do not obey simple asymptotic relations. The present linear δ Scuti models predict very dense frequency spectrum which does not explain the observational facts, i.e. the limited number of excited modes above the observable level of amplitudes. It is generally accepted that some mode selecting and/or amplitude limiting mechanisms caused by nonlinearity are missing from the present models.

As Pamyatnykh at al. (1998) wrote: "it is clear that improvement on the side of theory is needed before we will be able to produce a credible seismic model" of a δ Scuti star and mode identification remains impossible unless we discover the clue to mode selection. They urged that observational determination of *l* values for some of the excited modes could significantly change the situation.

It has been discussed by many authors (Dziembowski 1977; Balona & Stobie 1979; Stamford & Watson 1981; Watson 1988; Garrido et al. 1990; Garrido 2000) that multicolour photometry contains information about *l* because local temperature, geometry, pressure and limb-darkening variations are important contributing factors to the predicted flux changes.

However, the location of theoretical modes on the comparison plane is based on assumed ranges of (R, Φ_T) which are very uncertain. *R* is a parameter which describes departure from adiabacity of the atmospheres of pulsating stars. Φ_T phase lag gives the angle between maximum temperature and minimum radius.

In the past few years new theoretical investigations concerning the effect of rotation (Soufi et al. 1998) and limb-darkening (Heynderickx et al. 1994) for mode indentification have been carried out. Cugier et al. (1994) found that nonadiabatic observables are useful not only to determine *l* but also the radial order of the observed modes. It is a fact that this statement is deduced for β Cep stars, where the mode identification has a different problem based mostly on amplitude ratios, not phase differences.

Since mode identification of stars cannot be done independently of calculations involving construction of equilibrium models and their oscillation properties, all of the theoretical investigations are very important to find a final solution for mode identification. However, we definitely need additional guide-

Send offprint requests to: M. Paparó (paparo@ogyalla.konkoly.hu)

⋆ Based on observations obtained at the South African Astronomical Observatory, Sutherland, South Africa and at the European Southern Observatory, La Silla, Chile (Program 51 - 7 - 038)

⋆⋆ Research Director, Belgian Fund for Scientific Research (FWO)

lines to reduce the number of suitable models to a unique solution.

In the past few years many attempts have been carried out to obtain reliable criteria for mode identification from observational point of view in δ Scuti stars. As a most plausible solution the observable level of amplitude of the excited modes, based on remarkably longer data sets, were decreased to have more numerous excited modes above the observable level. While the problem is rather complex in matching the observed modes by theoretical models, considerable progress has been achieved as shown by Breger et al. (1995) and Guzik et al. (1998).

A promising tool is a search for regular frequency spacing. Of course, for low-overtone pulsators as δ Scuti stars, one cannot expect to find the asymptotic frequency spacing. However, the deviations from a regular frequency spacing are small even for low radial overtones and so some regularity among the pulsation modes excited to visible amplitude (Handler et al. 1997, Breger et al. 1999) can be expected. Beside the traditionally accepted line profile analysis (both time series or moment method) as a pure spectroscopic method for mode identification, a new complex method (equivalent width method) based on similtaneous observation of selected absorption lines combined with simultaneous photometric observations, has been established (Kjeldsen et al. 1995, Bedding et al. 1996) and applied to FG Vir (Viskum et al. 1998).

A common, pure multiphotometric method of determining the mode for δ Scuti stars is to plot amplitude ratio versus phase difference for two colours. According to Balona & Evers (1999) it is difficult to combine results from numerous two-colour diagrams. They improved a rigourous, statistically based, method of deducing the mode which does not require these plots and which gives the probability of correct identification for δ Scuti stars. A similar method has been proposed by Fontaine et al. (1996) for white dwarfs where only the amplitude dependence on wavelength is sensitive to the mode.

In the present paper we modify the common multiphotometric method of determining the mode for δ Scuti stars. On the basis of extended multisite, multiphotometric observations not only the generally used plane (A_{b-y}/A_y versus ϕ_{b-y} - ϕ_y) but each combination of the nonadiabatic observables including amplitude ratio vs. amplitude ratio and phase difference vs. phase difference planes are checked for observational guidelines to mode identification.

Additional information on data comparing to Paparó et al. 1996 (Paper I) and Sterken 1997 (Paper II) is discussed in Sect. 2. Nonadiabatic observables (amplitudes and phases) with their error bars are presented in Sect. 3. The most useful set of plots for observational guidelines to mode identifications are shown in Sect. 4. A discussion concerning the conclusion of plots is given in Sect. 5.

2. The new data

We refer to Paper I for details on the instrumentation and journal of observations. The *u*,*v* and *b* magnitudes (1450 observations for each colour) collected simultaneously with the *y* magnitudes using SAT *uvby* photometer in Chile are discussed in Paper II. The new data in the present paper are 460 *b* magnitudes using the single-channel photometer attached to the South African Astronomical Observatory 0.5 m telescope at Sutherland during 13 nights obtained by M. Paparó. The reduction procedure, including a check for constancy of comparisons, homogenization of data and investigation of mean light level of θ Tucanae, was the same for each colour as it is described in Paper I. The magnitude difference between the comparison stars, $\Delta b_{SAAO} = -1.4306 \pm 0.0032$ and $\Delta b_{ESO} = -1.4303 \pm 0.0038$, shows the constancy of comparisons in *b* colour, too, and the fact that the zero point of the SAAO and ESO instrumental Strömgren systems are close to each other in *b* without any transformation. Nevertheless, because of the homogeneous treatment of colours a similar zero point shift procedure was applied for the SAAO *b* data as it is described in Paper I for *y* colour. The photometric zero-point of ESO system is accepted as the zero-point of the homogeneous *b* data set. For the different light curves an adjustment

$$\mathrm{ESO} = \mathrm{SAAO} + 0.00829$$

and for the differential light curve of comparisons an adjustment

$$\mathrm{ESO} = \mathrm{SAAO} + 0.00154$$

were accepted in *b*. After the zero-point shift the SAAO and ESO *b* mean light level values outline the same curve as it is shown in Fig. 2a of Paper I for *y*. The colour changes through the orbital cycle have been discussed in detail in Paper II and shown in Fig. 5. The *v* and *u* data were left in the ESO instrumental system. Our following analysis and results are based on more than 2300 y, almost 2000 *b* and *b-y* and almost 1500 *u* and *v* measurements which were treated homogeneously resulting in a homogeneous data set.

3. Nonadiabatic observables

We follow the terminology of Cugier et al. (1994) used in β Cephei models. They adopted the term *nonadiabatic observables* to denote amplitude ratios and phase difference for any pair of oscillating parameters such as light in a selected filter, colour or radial velocity. They believe that in addition to precise frequency measurements, the nonadiabatic observables should be regarded as important data for asteroseismology.

A multifrequency analysis of θ Tucanae photometry was performed with the MUFRAN program (Kolláth 1990) and described in detail in Paper I. Ten pulsational frequencies were found in the range of 15.86 to 20.28 cycles/day. Two frequencies (0.282 and 0.142 cycles/day) were found to be responsible for the mean light level variation of θ Tucanae. A third frequency at 0.99350 cycles/day having 1.9 mmag amplitude near the level of significance was also found in the low frequency region. It could be a sign of a not-perfect homogenization, although the coincidence of the nightly mean value of θ Tucanae obtained at different sites with a periodic curve suggests no problem involved in the homogenization. Regarding the 1.00 $(f_4 - f_3)$ and 0.957 $(f_5 - f_4)$ cycles/day frequency differences between three

pulsational frequencies, the frequency at 0.99350 cycles/day may be due to a linear combination of f_3, f_4 and f_5 which is not properly resolved. In a simulation noiseless synthetic data were generated for the three sinusoides mentioned above with data points distributed in time according to the observational data. A single peak at 0.99904 cycles/day revealed in the low frequency domain confirming our guess for the two unresolved linear combinations.

Nevertheless, in the present paper the 13 frequencies, worked out in Paper I were accepted and used to get the nonadiabatic observables for θ Tucanae. In Table 1 amplitudes and phases of the 10 pulsational frequencies for each Strömgren bands and colour indices are given, respectively, in mmag and degrees. The amplitudes and phases were obtained by least squares solution. With this solution a synthetic light curve was calculated. Noise was generated 300 times by a random number generator and added to the synthetic light curve. The parameters were determined in each case. Errors in amplitudes and phases are given as standard deviation around the mean value.

We would like to call the attention that such kind of error calculation gives only the error bar of finding the frequencies because of observational errors. As the stability investigation for θ Tuc (Paparó 2000) shows, larger uncertainties are involved in the solutions because of the length and distribution of data. The SAAO and ESO data were separately treated. Amplitudes and phases for both data sets can be found in Tables 1–4 of that paper.

Determination of amplitudes and phases for the 13 frequencies were given in Table 2 in Paper II using only the ESO colour data. The amplitudes in *v* and *u* are the same as here because the same data set was used. In *y* and *b* the increased amount of data resulted in different values for the *y* and *b* amplitudes.

The phases differ in Paper II and the present paper because a different epoch was used. In the present calculation only the last four digits of HJD integer were applied and the HJD integer of the first observation, 9249, was used as an epoch. Since the phase differences between colours and colour indices are independent of the epoch, the accepted value does not play a special role.

The colour dependence of amplitudes and phases based on ESO colour data was discussed in Paper II and shown in Fig. 3. A common trend was pointed out namely that the amplitudes of the frequencies $f_3 - f_{12}$ increase towards shorter wavelengths.

As a more sophisticated check based on the error bars of the present investigation shows three modes (f_3 = 17.06289, f_6 = 15.86246 and f_9 = 15.94618) having unusual behaviour in *u* colour compared to the common trend for other modes. *These modes have lower amplitude in u than in v.* For two modes (f_3 and f_9) not only the amplitude values are lower but even the error bars are separated. Model calculations for the variation of amplitude ratio in different passbands (Balona & Evers 1999 and Garrido 2000) also show a break down in the short wavelength.

Table 1 is used to calculate the value of the nonadiabatic observables, amplitude ratios and phase differences. A non-correlated error calculation was carried out for the error bars of nonadiabatic observables.

For amplitude ratio A_b/A_y, for example,

$$\sigma_{A_b/A_y} = \sqrt{[(\sigma_{A_b}/A_b)^2 + (\sigma_{A_y}/A_y)^2] * (A_b/A_y)^2} \quad (1)$$

and for phase difference ϕ_b - ϕ_y

$$\sigma_{\phi_b - \phi_y} = \sqrt{\sigma^2_{\phi_b} + \sigma^2_{\phi_y}} \quad (2)$$

equations were applied where A_y, A_b are the amplitude values, $\sigma_{A_y}, \sigma_{A_b}$ the corresponding errors from Table 1a. σ_{ϕ_b} and σ_{ϕ_y} are the errors of the phases in the given colours from Table 1b. For the most important nonadiabatic observables served as useful criteria the values and error bars are given later in Table 5. These calculations and the sophisticated results give a strong base for searching observational guidelines for mode identification for θ Tucanae based on multicolour photometry.

4. Observational guidelines for mode identification

Each mode excited in a pulsating star is characterized by three quantum numbers. The process of determining *l*, *m* and *n* is known as mode identification. The azimuthal quantum number (*m*) is mostly obtained from spectroscopic observations. The horizontal quantum number (*l*) and the radial order (*n*) can be found from photometric observations.

Many authors (Watson 1988; Stamford & Watson 1981; Cugier et al. 1994; Garrido et al. 1990; Breger et al. 1999; Balona & Evers 1999 and Garrido 2000) discussed which are the best choices of filter bands for getting nonadiabatic observables. In principle, a relatively large baseline in wavelength is suggested. The light of different wavelengths comes from different radial layers of the star. The limb-darkening has a different effect for light of different wavelengths. The nonadiabatic observables based on a larger baseline in wavelength contain more information about the star. However, because of practical observational reasons Johnson *B, V* and Strömgren *b, y* colours are most commonly used for mode identification.

Although we have *uvby* colours of θ Tucanae, the most important part of our investigation is based on only *b, y* colours and *b-y* colour index. A conclusion of the stability test by Paparó (2000) suggests that our almost 1500 *u, v* data give criteria for mode identification only in a limited way. It seems that neither the SAAO nor the ESO data are long and properly distributed enough to get a stable solution for the nonadiabatic observables. As soon as we put the two data sets together we step over the critical length and distribution of the data in respect to the given frequency spectrum of θ Tucanae and from the stable solution the correlations between the nonadiabatic observables reveal. The phrase *stable solution* is used in the present paper if the solutions of Fourier parameters (frequencies, amplitudes and phases) are the same within the error bars for two distinct data sets or for a shorter and longer data sets.

The first result that we should like to emphasize is that how important the critical length and distribution of data are in a given mode identification. In the past the mode identification of stars with complex frequency spectrum perhaps failed because

Table 1. Amplitudes and phases of 10 excited pulsational modes of θ Tucanae in different colours and colour indices.

Table 1a. Amplitudes of excited modes of θ Tucanae

	Frequency	A_y mmag	A_b mmag	A_v mmag	A_u mmag	A_{b-y} mmag	A_{v-b} mmag	A_{u-v} mmag	A_{c1} mmag	A_{m1} mmag
f_3	17.06289	5.18±.14	7.05±.18	9.11±.34	8.48±.40	1.30±.10	1.64±.15	1.64±.31	3.07±.40	0.49±.23
f_4	18.06302	4.96±.15	5.00±.20	5.87±.37	6.28±.44	1.07±.11	0.98±.17	1.73±.36	2.13±.45	0.42±.24
f_5	19.02045	5.01±.14	6.11±.16	6.57±.21	7.14±.24	1.11±.09	1.02±.10	1.39±.18	1.75±.24	0.64±.14
f_6	15.86246	3.82±.15	5.06±.15	6.06±.21	6.00±.25	1.00±.09	1.04±.10	1.12±.16	1.79±.22	0.31±.12
f_7	20.28061	15.16±.14	18.52±.15	20.79±.19	24.27±.22	3.14±.08	2.43±.09	4.18±.17	2.93±.22	1.06±.13
f_8	19.79407	3.97±.14	4.66±.15	5.27±.20	5.39±.23	0.81±.09	0.63±.09	0.80±.15	1.02±.21	0.36±.13
f_9	15.94618	3.98±.15	5.24±.16	6.14±.21	5.56±.25	1.06±.09	1.06±.10	0.95±.18	1.90±.24	0.25±.12
f_{10}	20.11136	5.38±.15	6.54±.16	7.71±.22	8.27±.26	1.06±.10	0.96±.10	0.98±.18	1.21±.25	0.42±.15
f_{11}	17.54177	1.94±.13	2.04±.14	2.23±.17	2.34±.20	0.41±.08	0.45±.08	0.25±.14	0.55±.19	0.49±.12
f_{12}	17.85665	1.73±.13	1.84±.14	1.87±.19	1.89±.23	0.37±.08	0.23±.08	0.64±.17	0.84±.23	0.51±.14

Table 1b. Phases of excited modes of θ Tucanae

	Frequency	φ_y deg	φ_b deg	φ_v deg	φ_u deg	φ_{b-y} deg	φ_{v-b} deg	φ_{u-v} deg	φ_{c1} deg	φ_{m1} deg
f_3	17.06289	16.1±1.6	6.5±1.6	3.7±2.3	13.1±2.8	5.1±4.7	346.9±5.8	127.3±11.0	148.5±7.9	288.3±34.6
f_4	18.06302	55.6±1.8	52.7±2.4	40.4±3.9	54.9±4.3	62.4±6.2	27.8±10.9	123.7±10.9	153.1±12.6	319.5±45.6
f_5	19.02045	99.4±1.6	105.5±1.5	104.3±1.8	114.1±1.9	111.8±4.6	83.5±5.2	172.2±7.7	208.5±7.9	355.9±13.4
f_6	15.86246	107.5±1.9	108.0±1.5	106.8±1.7	117.1±2.1	115.2±4.2	94.4±4.7	203.2±9.8	237.6±7.8	1.5±29.5
f_7	20.28061	11.1±0.5	7.9±0.5	6.3±0.5	12.2±0.5	5.5±1.5	358.7±2.0	42.2±2.3	77.3±4.4	205.5±7.0
f_8	19.79407	332.3±1.8	328.1±1.7	324.9±1.9	333.0±2.2	336.4±5.4	314.1±7.5	47.3±12.4	84.2±12.4	181.6±22.5
f_9	15.94618	266.4±2.0	267.9±1.6	266.0±1.8	273.5±2.4	264.8±4.4	260.0±4.8	39.8±11.2	62.2±7.1	175.1±40.0
f_{10}	20.11136	276.5±1.5	271.7±1.3	271.1±1.5	277.2±1.7	269.1±4.5	251.6±5.6	331.1±11.5	21.9±12.2	118.2±23.2
f_{11}	17.54177	160.1±3.7	153.8±3.8	146.9±4.4	152.1±4.9	159.7±10.7	108.2±10.3	202.7±45.8	258.1±24.0	41.2±14.2
f_{12}	17.85665	194.6±4.6	204.6±4.6	210.3±6.0	230.0±6.7	226.5±12.3	152.2±23.9	300.4±16.1	309.6±16.3	83.6±15.0

of the unstable solution of nonadiabatic observables, not because of the small baseline in wavelength. The statistical method of Balona & Evers (1999) can be regarded as a bridge over the unstable solutions. However, combining the different colours in a statistical method we lose part of the information coming from different layers of the star.

In the present investigation we check the planes of nonadiabatic observables based on small baseline in wavelength but the solutions are stable for the whole data set of the multisite campaign.

A speciality of the present investigation is that not only the traditionally suggested (Watson 1988 and Garrido 2000) planes but each combination of the nonadiabatic observables including phase difference vs. phase difference planes were checked for observational guidelines.

A search for any kind of correlations between the nonadiabatic observables was carried out. Any definite, regular structure of the planes was recognized but only the higher level structures are presented. We do not mention the planes where no definite structures were noticed.

4.1. Straight lines

Distribution of points along a straight line used to be regarded as a definite correlation between parameters investigated. The straight line structure for different nonadiabatic observables is presented in Fig. 1. Symbols are interpreted in the next paragraph. Mostly the same kind of nonadiabatic observables, amplitude ratio vs. amplitude ratio or phase difference vs. phase difference for different colours, distribute along a straight line in our investigation. The modes along the straight lines do not show any systematic arrangements in the different panels except the first one. We should call, however, attention to two facts. Each graph presented in Fig. 1. includes parameters in *u* or *v* colours which are the least precisely obtained observables. Furthermore, graphs are presented in the paper by Paparó (2000) where distribution of modes along straight lines are caused by the unstable solution of nonadiabatic observables as a consequence of inproper data sets. We present these straight lines as examples which are not suggested to be used for any kind of conclusion in mode identification.

4.2. Groups

The second definite structure that we noticed is the group of modes. We call the closely spaced modes a group if the error bars of the modes are practically distinct from the error bars of modes in another group. On the other hand the mean value of the closely spaced modes in a certain group differs from the mean value of the other group by more than 10% of the lower mean value. Of course the grouping is more definite if the scatter of modes around the mean value is smaller.

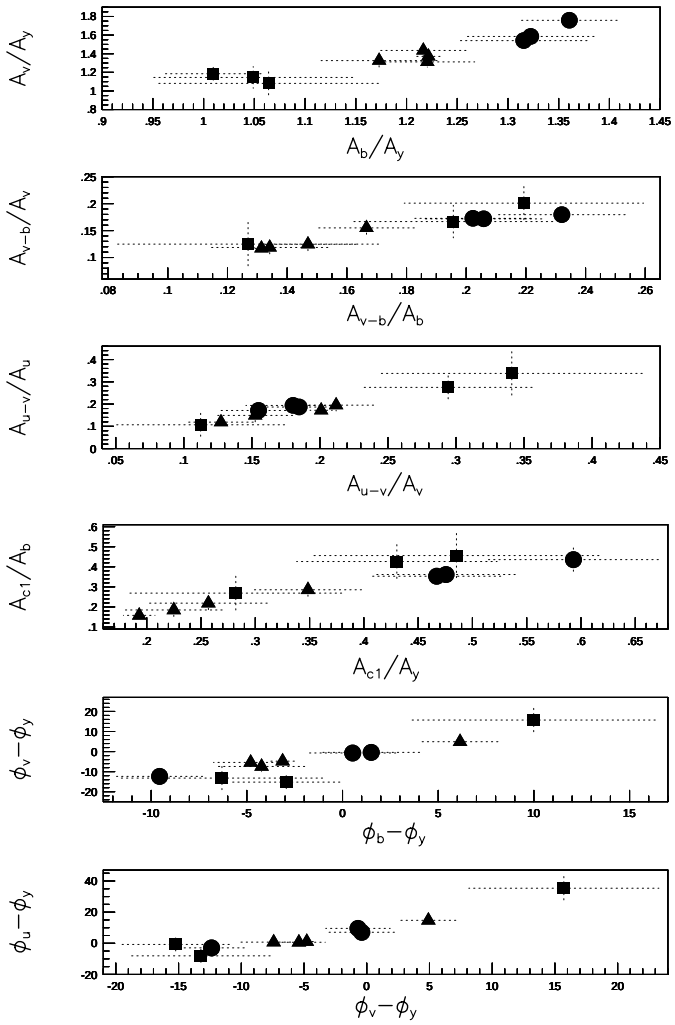

Fig. 1. Unstable solutions of amplitude ratios and phase differences are distributed along straight lines

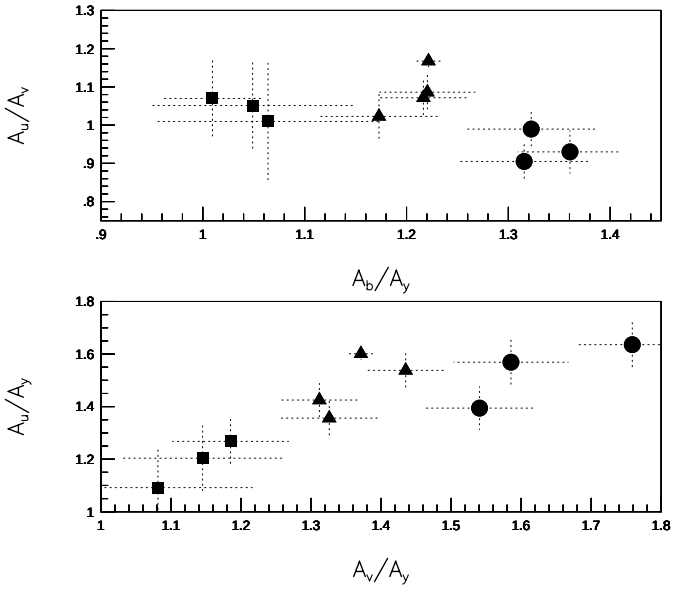

Fig. 2. Grouping according to A_b/A_y and unusual behaviour of modes of Group III in *u*

Table 2. List of modes in Groups. Values are given in cycle/day

Group I filled square	Group II filled triangle	Group III filled circle
18.06	20.28	15.86
17.54	19.02	15.94
17.85	20.11	17.06
	19.79	

Table 3. Mean value of amplitude ratio for the Groups

Groups	A_b/A_y	A_{b-y}/A_y	A_{b-y}/A_b	A_v/A_y	A_u/A_y	A_u/A_v
Group I	1.041	0.214	0.206	1.137	1.188	1.044
Group II	1.208	0.207	0.172	1.361	1.480	1.087
Group III	1.333	0.260	0.195	1.628	1.533	0.942

Both definite and looser groupings are presented in Fig. 2. *Three definite groups of modes exist according to A_b/A_y shown in the first panel*. The grouping of modes is so distinct, the scatter around the mean value is so small that the modes in a certain group are marked by the same symbol in each figure. It is supposed that the modes in a group have the same value for one of the quantum numbers and may have similar behaviour according to other nonadiabatic observables. The frequency values which belong to modes in a certain group and the symbols are listed in Table 2. These groups contain closely spaced modes not only according to A_b/A_y amplitude ratio but according to the frequency values. These modes are referred to in the rest of the paper as Group I, II and III.

The mean value of amplitude ratios involved in our graphs are given in Table 3 for each group. Error bars are not given here and in Table 4 since the error bar of the individual modes presented on each figure gives more severe constraint for the groups. Nevertheless, the numerical values confirm how definite is the grouping according to A_b/A_y amplitude ratio.

A more loose grouping of the same modes along a straight line according to A_v/A_y can be seen in the second panel of Fig. 2. The scatter of modes is larger around the mean value in a certain group but the mean values in Table 3 definitely show the grouping of modes.

Both panels of Fig. 2 contain information for the unusual behaviour of modes in *u* for Group III. In the first panel the A_u/A_v amplitude ratio is less than 1.0 while for the other modes this value is larger than 1.0. In the second panel there is a break in the straight line because of the lower A_u/A_y value of modes in Group III. Both panels obviously confirm the conclusion what we previously mentioned based on Table 1 namely, that modes in Group III have lower amplitude in *u* than in *v* colour. This can be seen also from the appropriate columns of Table 3.

A specific model calculation for θ Tucanae obtained by Luis Balona shows that A_v/A_u ratio is lower than 1.0 for modes with

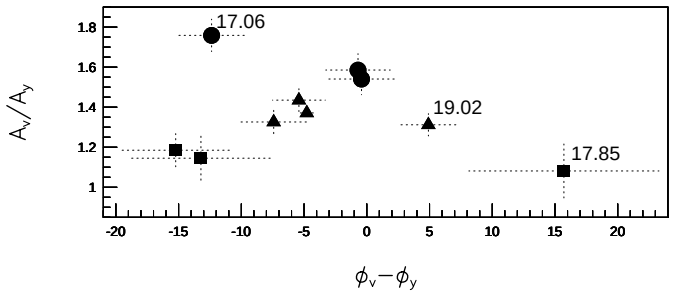

Fig. 3. Special arrangement of modes in A_v/A_y versus $\phi_v - \phi_y$ plane

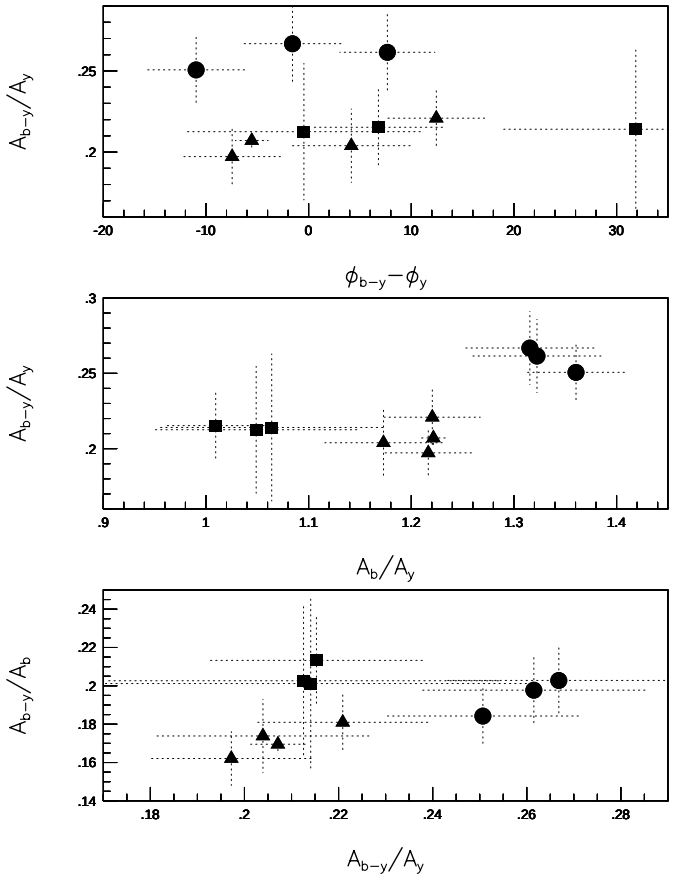

Fig. 4. Higher, distinct level of modes in Group III according to A_{b-y}/A_y

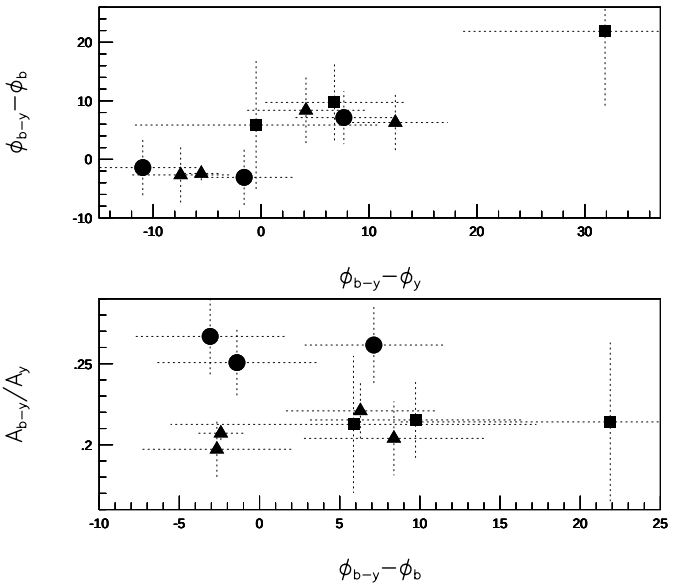

Fig. 5. Distinct level of modes according to $\phi_{b-y} - \phi_b$

larger frequency. However, Group III consists of modes with the lowest frequency values.

In Fig. 3 a special arrangement of modes on the A_v/A_y vs. $\phi_v - \phi_y$ plane can be seen. The grouping of modes according to $\phi_v - \phi_y$ is similar to the grouping based on A_b/A_y. However, one mode from each group has a special behaviour according to $\phi_v - \phi_y$ and they are situated on a crossing straight line or simply shifted according to $\phi_v - \phi_y$. The frequency values for the unusually behaving modes are given in the figure. Since the *v* colour data is shorter than *b* and *y*, the panel is worth showing because of the definite structure but no conclusion is given.

One axis of each panel in Fig. 4 shows the special behaviour of modes in Group III according to A_{b-y}/A_y. A higher, distinct level of A_{b-y}/A_y exists in the traditional plane used for mode identification. Modes in Group III display 25% higher mean values in A_{b-y}/A_y. It can be seen in the appropriate coloumn of Table 3. Group I and II are separated not only according to A_b/A_y but a slight separation according to A_{b-y}/A_b also seems to exist in the third panel of Fig. 4. Of course, the error bars of amplitude ratio including the colour index amplitude are larger because of the smaller amplitude variation in colour indices.

4.3. Levels

The third definite structures are the levels. The novelty of the present study is a check for correlation among the phase differences. Beside the traditionally used $\phi_{b-y} - \phi_y$, the $\phi_{b-y} - \phi_b$ phase difference proved to be a surprisingly good criterion for discrimination among the modes. We would like to emphasize at the first moment that both phase differences are obtained from a six-week long multisite campaign. The values plotted definitely belong to a stable solution.

In both panels of Fig. 5 the discriminative power of the $\phi_{b-y} - \phi_b$ phase difference is shown. In the first panel the location of modes on the plane of the two phase differences is given. It seems obvious that the $\phi_{b-y} - \phi_b$ phase difference is more discriminative for the modes than $\phi_{b-y} - \phi_y$. Along the $\phi_{b-y} - \phi_y$ axis the modes are continuously distributed, while according to $\phi_{b-y} - \phi_b$, two definite levels can be seen besides the third one. Since the third level contains only one mode (17.85 c/d) with the lowest amplitude among the frequencies, only the first two levels are mentioned as definite. It is worth mentioning that a certain level contains modes from different groups. The extention of error bar to the first level in the case of the first mode on the second level is acceptable since this mode (17.54 c/d) has one of the lowest amplitudes. Its amplitude is as low as for the single mode on the third level. Nevertheless, its

Table 4. Mean value of the phase differences for the levels

Levels	$\phi_{b-y}-\phi_b$ degrees	$\phi_{b-y}-\phi_v$ degrees	$\phi_{b-y}-\phi_u$ degrees
1.	-2.39	-0.65	-7.85
2.	+7.48	+10.06	+1.7
3.	+21.87	+16.15	-3.5

Table 5. Values and error bars of the most important nonadiabatic observables

Frequencies c/d	A_b/A_y	σ_{A_b/A_y}	$\phi_{b-y}-\phi_b$ degrees	$\sigma_{\phi_{b-y}-\phi_b}$ degrees
18.06302	1.01	0.06	9.73	6.62
17.54177	1.05	0.10	5.86	11.39
17.85665	1.06	0.11	21.87	13.13
19.79407	1.17	0.06	8.38	5.68
19.02045	1.22	0.05	6.29	4.78
20.28061	1.22	0.01	-2.41	1.58
20.11136	1.22	0.04	-2.66	4.65
15.86246	1.32	0.06	7.13	4.47
15.94618	1.32	0.06	-3.08	4.66
17.06289	1.36	0.05	-1.41	4.98

location on the second level is convincing. The mean values of the levels for different colours are given in Table 4.

The ϕ_{b-y} phase difference to ϕ_v and ϕ_u, respectively, is also checked but the error bars are larger and the structure is not so clear. The lower levels are similar to the panel for $\phi_{b-y}-\phi_b$ but the higher levels are not constant lines anymore but decreasing straight lines.

Keeping the traditionally used A_{b-y}/A_y amplitude ratio, the $\phi_{b-y}-\phi_b$ phase difference is used on the horizontal axis of the second panel. Not only the higher distinct level of A_{b-y}/A_y for modes in Group III can be noticed but the two vertical levels of modes according to $\phi_{b-y}-\phi_b$ is displayed. This new version of amplitude ratio vs. phase difference plane contains more information about the behaviour of modes to each other than the traditionally used plane shown in the first panel of Fig. 4.

No doubt that *the phase difference $\phi_{b-y}-\phi_b$ proves to be a new, useful criterion for mode identification*, at least in θ Tucanae.

In Fig. 6 the two strongest criteria, $\phi_{b-y}-\phi_b$ versus A_b/A_y are plotted. *The modes are obviously arranged, according to two parameters, on levels in groups.* The values and error bars of the two strongest criteria are given in Table 5. This plane can serve as an observational guideline for mode identification. Although it does not give the exact value of quantum numbers but predicts which theoretical modes must share the same behaviour. As we have previously mentioned a finding of the horizontal quantum number (*l*) and the radial order (*n*) based on nonadiabatic observables has theoretical base. The two parameters in Fig. 6 may be the radial order (*n*) and the spherical harmonic degree (*l*). Following the theoretical predictions for δ Scuti stars the phase difference gives the horizontal quantum number of modes. A_b/A_y amplitude ratio gives the amplitude

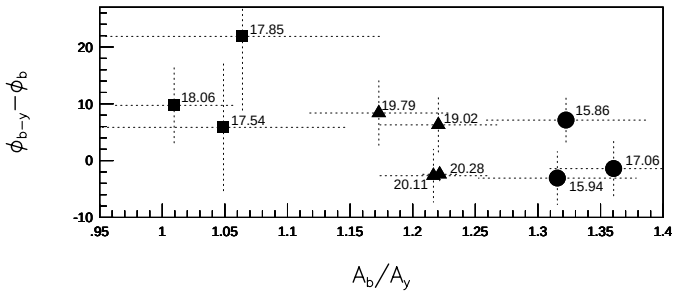

Fig. 6. Groups and levels according to the two strongest observational criteria, A_b/A_y and $\phi_{b-y}-\phi_b$. Discriminative plane for mode identification

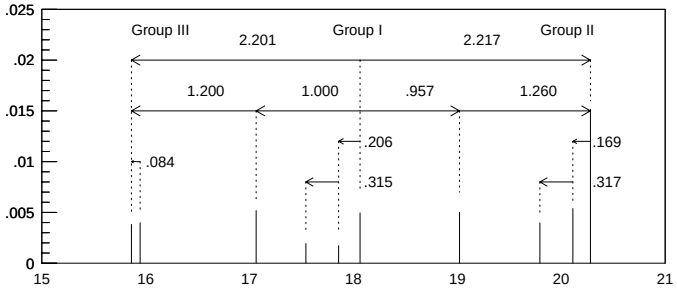

Fig. 7. Schematic frequency spectrum of θ Tucanae

ratio of eigenfunction in a different radial layer of the star. It is plausible to suppose that it gives information about the radial order of modes.

As we have shown in this paragraph observational guidelines for mode identification seem to exist for δ Scuti stars. These guidelines can help to reduce the number of suitable models to a unique solution. However, calibration of the pure observational guidelines by new, delicate theoretical calculation for planes of nonadiabatic observables concerning the location of theoretical modes is needed not only for *l* but with the radial order at the same time.

5. Discussion

We should summarize what we know about the 10 pulsational frequencies of θ Tucanae. For better understanding we reproduce here (Fig. 7) the schematic frequency spectrum of θ Tucanae published in Paper I. The extremely high regularity of frequency spacing is obvious. The spectrum is dominated by groups of closely spaced frequencies. The groups seem to be equally spaced and are divided by single frequencies.

According to A_b/A_y we distinguish three groups in the present investigation. The middle group on Fig. 7 corresponds to Group I. The (right side) higher frequency group and the single frequency correspond to Group II. Group III consists of the (left side) lower frequency group and the single frequency.

Modes in Group III have speciality in *u* colour and in A_{b-y}/A_y amplitude ratio. The modes have lower amplitude in *u* colour and higher A_{b-y}/A_y amplitude ratio than the modes in other groups. The A_b/A_y amplitude ratio is the highest for Group III, although Group I and II have increasing A_b/A_y am-

plitude ratio with increasing frequency. Since Group III does not show any special behaviour in A_{b-y}/A_b, the modes have to have smaller amplitude in *y* or larger amplitude in *b* than the other groups. Group I and II are slightly separated according to A_{b-y}/A_b.

Concerning the special behaviour of modes in Group III it would be a logical conclusion that these modes are excited in the secondary component of higher temperature in the binary system. Unfortunately, no spectral type has been obtained for the secondary component. However, the low mass $\approx 0.2M_\odot$ obtained from spectroscopy (Sterken et al. 1997) seems to exclude δ Scuti type pulsation in the secondary. Furthermore, the similar regularity in frequency spacing to the other modes would be a hard job to explain if we do not involve a very severe tidal synchronization in the oscillation.

If these modes belong to θ Tuc, serious questions can be raised. Can we find a region of excitation with higher temperature and/or nonadiabacity (larger α_T) what we need to explain the higher A_{b-y}/A_y amplitude ratio of modes in Group III? According to the present theoretical point of view the region of excitation is indifferent in respect of the observable behaviour of modes. A new investigation of the location of theoretical modes on the traditional comparison plane based on the actual model atmospheres has been recently published by Garrido (2000). For *l* = 3 the amplitude ratio A_{b-y}/A_y is very different (much higher) from the lower *l* - values. Should we identify the modes in Group III with *l* = 3 value? Such a straightforward conclusion does not seem to be well-established since the present paper gives the arrangement of modes according to two parameters simultaneously not only according to *l*.

In fact, the behaviour of the 10 pulsational modes on the levels seems to be unified. The modes in Group III join the same levels as the other modes. Not all modes in a group belong to the same level. This is a normal behaviour if we see groups connected to the radial overtones. According to the modelling of θ Tucanae by Templeton et al. (2000) the frequency distances between the consecutive low radial orders of the radial modes are $\approx$ 2.9 c/d for most of the models. However, the distances between the non-radial consecutive radial orders show variety of values from 2.9–1.6 cycles/day for Models 1–3 and 2.85–0.55 cycles/day for the Model 4. In the observation the dominant frequency spacing is 2.2 c/d.

In our view the sign of $\phi_{b-y} - \phi_b$ is opposite to the sign of $\phi_{b-y} - \phi_y$. As a first approximation, the first level with $-2.^o39$ mean value is regarded as the location of radial modes *l = 0*, while the *l = 1* modes are situated on the second level. The third level corresponds to *l = 2*. The groups would be the consecutive radial orders.

However, such an explanation creates some problem. There are pairs of modes with the same radial quantum number situated on the same level. It is obvious, especially for the closely spaced frequencies, that such a simple interpretation does not work. These modes may not be consecutive radial orders with the same *l* value. There are two ways of avoiding the duplicating of modes.

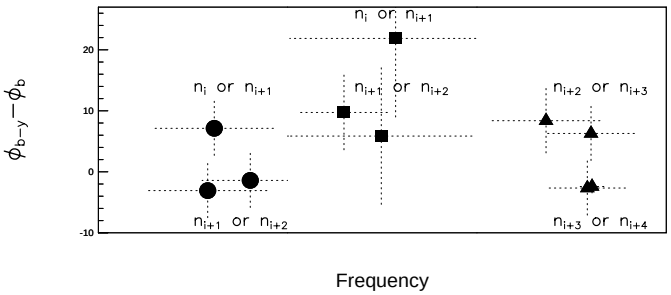

Fig. 8. Systematics in radial orders for θ Tucanae

1.) In the first explanation the duplicating of modes with the same radial and horizontal quantum numbers are caused by rotational splitting. In this case the member of pairs have different azimuthal quantum number (*m*). However, the values of splitting are remarkably different (1.12, 0.169, 0.77 and 0.52 c/d) for the different pairs and only two modes are seen instead of tripletts. More serious problem that the rotational splitting explanation does not work for the radial modes on the first level. Two of the modes (17.06 and 19.02 c/d) behaving unusually according to $\phi_v - \phi_y$ on Fig. 3 are involved in pairs on the first and second levels.

The pair of 20.11 and 20.28 c/d should be separately mentioned since it is connected to a unique effect. On the upper panel of Fig. 8 in the paper by De Mey et al. (1998) a *node seems to exist for the mode at 20.28 c/d*. However, in the model calculations the outermost mode is located in much deeper layers even for high overtones. The layers (temperature is above 2x10^5 ^oK) cannot be reachable by spectroscopic observations. A preliminary mode identification of θ Tucanae matching the observed and rotationally splitted theoretical modes has been recently published by Templeton et al. (2000). This mode is *supposed* to be a radial mode and the best fit is the fourth overtone. It is worth mentioning that this is the dominant mode of θ Tuc with the largest amplitude.

2.) In the second explanation we suppose that the levels give information only for the even (including zero) and odd consecutive *l* value of modes. The first level contains both *l = 0* and *l = 2* modes, while the second level contains modes with *l = 1* and *l = 3*. According to the asymptotic theory *l = 0* and *l = 2* further *l = 1* and *l = 3* modes, respectively, are closely spaced in frequency. However, what is the explanation for the third level in this scenario, *l = 4* and *6*? In the identification of Templeton et al. (2000) the two frequencies at 15.86 c/d and 15.94 c/d *l* = 2 *n* = 1 and *l* = 2 *n* = 2 values are given, respectively. In our figure these modes are situated on different levels. The identification of 15.94 c/d mode can be accepted but for 15.86 c/d *l* = 3 or 1 would agree with our discriminative plane.

The third level is connected to a hitherto not mentioned but interesting fact. The unusually behaving modes according to $\phi_v - \phi_y$ on Fig. 3 (marked by asterisk in Table 6) are situated on three different levels and are different overtones. Two of them represent the single modes between groups in Fig. 7. The role of these modes is not clear. However, the frequency at 19.02 c/d

Table 6. Possible schematic and numerical identification of modes in θ Tuc. The numerical values (marked as particular) are based on the second explanation if we accept the identification of 20.28 c/d given by Templeton et al. 2000 (Frequency f, $1.)$ first explanation, $2.)$ second explanation.

	$1.)$		$2.)$ general		$2.)$ particular	
f	*n*	*l*	*n*	*l*	*n*	*l*
15.86	n_i	*1*	n_i or n_{i+1}	*3* or *1*	*1* or *0*	*1* or *3*
15.94	n_i	*0* and ?	n_{i+1} or n_{i+2}	*2* or *0*	*2*	*2*
17.06*	n_i	*0* and ?	n_{i+2} or n_{i+1}	*0* or *2*	*3*	*0*
17.54	n_{i+1}	*1* and m_i	n_{i+2} or n_{i+1}	*1* or *3*	*2*	*1*
17.85*	n_{i+1}	*2*	n_i or n_{i+1}	*4* or *6*	*1* or *0*	*4* or *6*
18.06	n_{i+1}	*1* and m_{i+1}	n_{i+1} or n_{i+2}	*3* or *1*	*1*	*3*
19.02*	n_{i+2}	*1* and m_i	n_{i+3} or n_{i+2}	*1* or *3*	*3*	*1*
19.79	n_{i+2}	*1* and m_{i+1}	n_{i+2} or n_{i+3}	*3* or *1*	*2*	*3*
20.11	n_{i+2}	*0* and ?	n_{i+3} or n_{i+4}	*2* or *0*	*3*	*2*
20.28	n_{i+2}	*0* and ?	n_{i+4} or n_{i+3}	*0* or *2*	*4*	*0*

exhibit strong g-mode type behaviour according to Templeton et al. (2000).

The following principles can help in the interpretation of the radial order. According to the asymptotic theory *P(l, n)* ≈ *P(l+2, n-1)* relation is valid. If a pair exists in a group on a certain level the radial order has to be consecutive values. The radial orders in the same group but on different levels are shifted to each other by one consecutive radial order. The first level has the highest radial orders, the other levels have lower and lower values. The consecutive groups in frequency have consecutive radial orders decreasing to the direction of lower frequency. Fig. 8 gives the systematic arrangement of radial orders in this concept for θ Tucanae. The groups are rearranged here according to increasing frequency but the location of modes to each other are kept as in the discriminative plane. Surprisingly simple arrangement of radial orders revealed. The rotational splitting is not involved in this explanation.

According to the logical-theoretical calibration of Fig. 6 the possible schematic identification of modes are given in Table 6. n_i, n_{i+1}, n_{i+2} and n_{i+3} mean consecutive radial orders, m_i and m_{i+1} are different azimuthal order of rotationally splitted modes. The first column gives the frequencies. The 2 and 3 columns (marked as $1.)$) give the result of the first explanation, the 4 and 5 columns (marked as $2.)$) give the possible solution of the second explanation in general.

If we accept the *l = 0, n = 4* identification of the frequency at 20.28 c/d given by Templeton et al. (2000) the resulting particular identification of modes based on the systematics are given in the last two columns of Table 6.

The exact calibration of the observational guidelines obtained in this investigation is definitely needed. How general the regularities are for other stars we do not know at this moment. How these regularities would be confirmed or modified by regularities in *v* and *u* we also do not know. How these regularities are really connected to the quantum numbers (*l, n* and *m*) is a future task of detailed theoretical modelling. However, we can find some connection to investigations published in the literature.

Grouping in modes of FG Vir according to the $A(H_\alpha)/A(FeI)$ parameter has been published by Viskum et al. (1998). The modes in a group are interpreted as modes with the same *l* value comparing to other mode identification methods. However, one problem arises immediately. In the group *l = 0* two modes are too closely spaced in frequencies for both to be radial modes. It is maybe the same duplicating effect what we have on the levels in our investigation. Fig. 6 of that paper can be an example for our interpretation concerning the stability of solution. The grouping of modes disappears, the modes are distributed along a straight line, as part of the data has been excluded. The stability of the solution is questionable for this particular data set.

Only a few published examples are mentioned but in the near future another δ Scuti star (38 Eri) is going to be investigated by one of the authors (MP) following the concept of the present investigation.

The high level systematic behaviour of the observational facts in θ Tucanae concerning both the regularities in frequency spacing, in grouping according to amplitude ratios and in leveling according to phase differences, give high probability to reduce the number of suitable models to a unique solution. The observational guidelines, hopefully, can serve as key to the mystic mode selecting and/or amplitude limiting mechanism in low amplitude δ Scuti stars.

Acknowledgements. Hungarian research grant, OTKA No. T 025288, and financial support of Soros Foundation are acknowledged. MP acknowledges South African Astronomical Observatory (SAAO) for observing possibility and hospitality of staff members. Thanks to Dr Géza Kovács for running his program on error calculation. We are thankful to Dr Luis Balona for his specific model calculation. Fruitful discussions with Prof. Hiromoto Shibahashi, Drs Béla Szeidl and Zoltán Kolláth are highly appreciated. CS acknowledges financial support from the Belgian Fund for Scientific Research (FWO) and ESO for granting a generous amount of observing time (Period 51). The authors are indebted to Dr A.A. Pamyatnykh for his valuable remarks in his referee report.

References

Balona L.A., Evers E.A., 1999, MNRAS 302, 349
Balona L.A., Stobie R.S., 1979, MNRAS 189, 649
Bedding T.R., Kjeldsen H., Reetz J., Barbuy B., 1996, MNRAS 280, 1155
Breger M., Handler G., Nather R.E., et al., 1995, A&A 297, 473
Breger M., Pamyatnykh A.A., Pikall H., Garrido R., 1999, A&A 341, 151
Cugier H., Dziembowski W.A., Pamyatnykh A.A., 1994, A&A 291, 143
De Mey K., Daems K., Sterken C., 1998, A&A 336, 527
Dziembowski W., 1977, Acta Astron. 27, 203
Fontaine G., Brassard P., Bergeron P., Wesemael F., 1996, ApJ 469, 320
Garrido R., 2000, In: Breger M., Montgomery M.H. (eds.) Delta Scuti and Related Stars. ASP Conf. Ser. in press
Garrido R., Garcia-Lobo E., Rodriguez E., 1990, A&A 234, 262

Guzik J.A., Templeton M.R.,, Bradley P.A., 1998, ASPC 135, 470
Handler G., Pikall H., O'Donoghue D., et al., 1997, MNRAS 286, 303
Heynderickx D., Waelkens C., Smeyers P., 1994, A&AS 105, 447
Kjeldsen H., Bedding T.R., Viskum M., Frandsen S., 1995, AJ 109, 1313
Kolláth Z., 1990, Occasional Technical Notes. Konkoly Obs. 1
Pamyatnykh A.A, Dziembowski W.A., Handler G., Pikall H., 1998, A&A 333, 141
Paparó M., 2000, In: Breger M., Montgomery M.H. (eds.) Delta Scuti and Related Stars. ASP Conf. Ser. in press
Paparó M., Sterken C., Spoon H.W.W., Birch P.V., 1996, A&A 315, 400 (Paper I)
Soufi F., Goupil M.J., Dziembowski W.A., 1998, A&A 334, 911
Stamford P.A., Watson R.D., 1981, Ap&SS 77, 131
Sterken C., 1997, A&A 325, 563 (Paper II)
Sterken C., De Mey K., Gray R.O., 1997, JAD 3, 3
Templeton M.R., Bradley P.A., Guzik J.A., 2000, ApJ 528, 979
Viskum M., Kjeldsen H., Bedding T.R., et al., 1998, A&A 335, 549
Watson R.D., 1988, Ap&SS 140, 255